AIAA AVIATION Forum
8-12 June 2026, San Diego, CA
AIAA AVIATION 2026 Forum

10.2514/6.2026-4266

Ultra-Wideband Sensor Fusion for Robust 3D Localization of Lighter-Than-Air UAVs

Samson Connelly[*], Matthew Widjaja[†], Andrew Meighan[‡], Paul Coen[§], Caeden Taylor[¶], and Or D. Dantsker[‖]
Indiana University, Bloomington, IN 47408

Abstract

Autonomous robotic systems operating in GPS-denied environments require accurate three-dimensional localization under practical hardware constraints. Current solutions use LiDAR and inertial measurement units to generate accurate position estimates while also mapping the local environment. However, these sensors and their associated processing requirements are not well suited to the strict size, weight, and power constraints of LTA vehicles. This paper presents a lightweight multi-sensor localization system for lighter-than-air (LTA) unmanned aerial vehicles operating under strict size, weight, power, and cost constraints. The proposed architecture integrates Ultra-Wideband (UWB) ranging, inertial measurements, and barometric altitude sensing using an Extended Kalman Filter. High-rate IMU measurements provide continuous state propagation, while asynchronous UWB range updates and barometric altitude measurements correct accumulated drift. The barometer improves vertical boundedness in a four-anchor UWB configuration, where altitude estimation is sensitive to anchor geometry and vertical observability. The system was implemented on a compact embedded platform with a total payload mass of 30.17 g. Experimental validation was conducted using a prescribed three-dimensional test trajectory in a GPS-denied indoor environment. Because time-synchronized absolute ground truth was not collected, performance was evaluated using deviations from the expected horizontal path and altitude bounds. The fused EKF solution achieved a mean horizontal radial error of 0.324 m, a mean vertical bound error of 0.010 m, and a mean combined trajectory-bound error of 0.327 m. These results indicate that lightweight UWB, inertial, and barometric sensing can maintain a bounded sub-meter three-dimensional position estimate suitable for autonomous coordination and navigation of LTA vehicles constrained by size, weight, and power.

Nomenclature

DTR	=	Defend the Republic competition
EKF	=	extended Kalman filter
IMU	=	inertial measurement unit
LTA	=	lighter-than-air
PCB	=	printed circuit board
RF	=	radio frequency
UAV	=	unmanned aerial vehicle
UWB	=	ultra-wideband
$a_{i,x}, a_{i,y}, a_{i,z}$	=	known three-dimensional coordinates of anchor i
$h(\mathbf{x})$	=	predicted measurement function
$h_i(\mathbf{x})$	=	predicted measurement function for UWB anchor i
H_{baro}	=	barometric measurement matrix

*Undergraduate Student, Deparment of Intelligent Systems Engineering, sambconn@iu.edu.
†Undergraduate Student, Department of Intelligent Systems Engineering, mawidj@iu.edu. AIAA Student Member.
‡PhD Student, Department of Intelligent Systems Engineering. ameighan@iu.edu. AIAA Student Member.
§PhD Student, Department of Computer Science. pcoen@iu.edu. Scientist, Naval Surface Warfare Center Crane Division. AIAA Student Member.
¶MS Student, Department of Intelligent Systems Engineering, caedtayl@iu.edu. AIAA Student Member.
‖Assistant Professor, Department of Intelligent Systems Engineering, odantske@iu.edu. AIAA Member.

$H_{uwb,i}$	=	UWB measurement Jacobian for anchor i
p_x, p_y, p_z	=	three-dimensional position coordinates
v_x, v_y, v_z	=	three-dimensional velocity components
$\mathbf{x}$	=	six-dimensional state vector
y_k	=	innovation, defined as the difference between measured and predicted values
z_{baro}	=	barometric altitude measurement
$z_{uwb,i}$	=	UWB range measurement from anchor i
σ_{baro}	=	barometric measurement noise parameter

I. Introduction

As the prevalence of autonomous unmanned aerial vehicles (UAVs) continues to increase, there is a growing demand for systems with sufficient onboard sensing and computation to complete dynamic tasks with minimal human interaction. Reliable localization is a fundamental requirement for these systems, particularly as vehicle autonomy and fleet size increase. As fleet size grows, the effectiveness of individual vehicles decreases without accurate localization, robust state estimation, and coordination between active vehicles. These challenges are especially important in GPS-denied environments, where autonomous vehicles cannot rely on satellite-based navigation and must instead estimate their motion and position using onboard sensing and local infrastructure.

At the Defend The Republic (DTR) competition, collegiate teams develop competitive lighter-than-air (LTA) vehicles under strict physical constraints. The DTR competition requires teams to operate within a GPS-denied environment while satisfying severe size, weight, and power limitations.[1,2] These constraints make the DTR environment a representative test case for practical GPS-denied autonomy, where localization systems must be accurate, lightweight, computationally efficient, and suitable for real-time deployment on small embedded platforms.

Current approaches to GPS-denied autonomous localization for DTR-style LTA UAVs often rely on vision-based algorithms that estimate vehicle position relative to objects with known locations.[3,4] While vision-based localization can be effective, its accuracy may be limited by field-of-view, lighting, occlusions, and line-of-sight constraints. Current industry-standard applications often use LiDAR and simultaneous localization and mapping to provide accurate spatial mapping;[5] however, these sensors and their associated processing requirements are not well suited to the strict size, weight, and power constraints of LTA vehicles.[6–9] LTA vehicles systems are strongly constrained by payload mass, power availability, and onboard sensing capacity, limiting the use of heavier or computationally intensive localization payloads.[6,7,10] As a result, there is a need for lightweight localization architectures that can maintain reliable three-dimensional state estimates without relying on GPS, high-power perception sensors, or external motion-capture systems.

Prior work in GPS-denied localization has explored Ultra-Wideband (UWB) ranging, inertial navigation, and sensor-fusion approaches. UWB is a wireless communication protocol that uses time-of-flight measurements to estimate the distance between a stationary anchor and a moving tag.[11,12] UWB ranging can provide accurate indoor distance measurements and is attractive for small UAV applications due to its relatively low mass, low power consumption, and modest computational requirements. However, UWB-based localization performance can degrade under non-line-of-sight propagation, multipath effects, poor anchor geometry, and unfavorable geometric dilution of precision.[12,13] These limitations are particularly relevant for compact four-anchor configurations, where anchor placement and the spatial distribution of anchor heights can strongly affect vertical observability and overall three-dimensional localization accuracy.[13,14]

Inertial Measurement Units (IMUs) provide a complementary sensing modality by enabling high-frequency dead reckoning through measured acceleration and angular velocity. An IMU can be used to propagate the vehicle state between external measurement updates; however, inertial sensor noise and bias errors accumulate through integration and cause drift in the estimated position, velocity, and orientation over time.[15,16] To address the limitations of standalone UWB localization and inertial dead reckoning, Extended Kalman Filters (EKFs) are commonly used to fuse prediction models with nonlinear sensor measurements.[17,18] In this structure, high-rate inertial measurements provide continuous state propagation, while external measurements such as UWB ranges periodically correct accumulated drift.

This paper presents a solution to GPS-denied 3D localization for an LTA vehicle using UWB ranging, inertial measurements, and barometric altitude sensing. The proposed system fuses UWB, IMU, and barometric measurements within an EKF. The IMU provides high-rate state propagation, while UWB range measurements periodically correct accumulated drift.[17,18] Although four anchors are sufficient for 3D trilateration, UWB localization accuracy is strongly affected by anchor geometry, geometric dilution of precision, and the spatial distribution of anchor heights.[13,14] Therefore, barometric pressure data is integrated into the EKF to improve vertical estimation and reduce altitude drift.[18,19] By incorporating barometric altitude sensing, the system improves vertical observability in a lightweight four-anchor UWB configuration while maintaining compatibility with the inherent constraints imposed by LTA platforms. The resulting system provides a lightweight, low-cost localization architecture designed for LTA vehicles. By combining complementary sensing modalities, the proposed system maintains continuous position estimation while reducing the drift and vertical observability limitations associated with standalone UWB or inertial localization. This work focuses on developing a lightweight sensor-fusion architecture that maintains sub-meter accuracy under strict size, weight, and power constraints, supporting autonomous operation of LTA vehicles in GPS-denied environments.

This work is organized as follows: Section II provides background on the DTR competition and localization in GPS-denied environments. Section III describes the system design and architecture, including the sensing hardware, embedded implementation, and EKF-based sensor-fusion framework. Section IV presents the experimental results and discussion, including comparison against a three-dimensional reference trajectory. Finally, Section V summarizes the conclusions of this work and details future directions for improving the localization system and extending its capabilities for autonomous LTA UAV operation.

II. Background

A. Defend The Republic LTA Competition

The Defend The Republic (DTR) competition challenges university teams to design, build, and operate a fleet of semi-autonomous LTA UAVs in a GPS-denied environment.[1,2] The competition requires vehicles to coordinate within a shared indoor arena while completing competitive tasks under limited sensing, computation, and actuation capabilities. Often described as a robotic version of Quidditch, the game requires teams to capture neutrally buoyant helium balloons and pass them through goals while also preventing opposing teams from scoring. The arena contains circular, square, and triangular goals, with each team's goals assigned a distinct color. Matches are divided into autonomous and manual-control periods, and fully autonomous scoring is worth significantly more than manual scoring. As a result, autonomous performance is strongly dependent on each vehicle's ability to estimate its three-dimensional position relative to the goals, game objects, arena boundaries, and other vehicles. Indiana University's LTA UAVs are shown in Fig. 1.

DTR imposes strict vehicle-level constraints that make localization especially challenging. Each vehicle is limited by a specified amount of helium and a maximum takeoff weight of 100 g. These constraints limit the sensing, computation, communication, and hardware payload that an LTA vehicle can carry onboard.[3,6,7,10] Consequently, localization approaches commonly used on larger UAVs, such as LiDAR-based mapping or computationally intensive vision systems, are difficult to deploy on DTR-style LTA platforms. The absence of GPS further increases the difficulty, requiring the vehicle to estimate its state using lightweight onboard sensors and local infrastructure. Thus, developing an accurate localization system for these vehicles requires careful optimization of sensors, hardware, and software to balance accuracy, update rate, robustness, and payload cost.

B. Localization in GPS-Denied Environments

GPS-denied localization is commonly addressed using local sensing modalities such as radio ranging, inertial navigation, vision, LiDAR, or combinations of multiple sensors. However, for LTA vehicles, localization methods must provide sufficient accuracy while remaining lightweight, low power, and computationally efficient. This motivates the use of UWB ranging, inertial measurements, and barometric altitude sensing as complementary sources of localization information.

Figure 1. Indiana University's LTA UAVs maneuvering through the arena during a DTR match.

Ultra-Wideband is a wireless radio frequency (RF) communication protocol that transmits short pulses containing data packets. UWB modules estimate range by measuring the time of flight of short radio packets between transmitting and receiving nodes.[11] For three-dimensional localization, stationary UWB modules, referred to as anchors, are placed at known coordinates, while a mobile UWB module, referred to as the tag, is mounted on the vehicle. With at least four anchors, the tag position can be estimated through trilateration. In this formulation, each measured range defines a sphere centered at the corresponding anchor, with the radius determined by the time-of-flight measurement. The tag location is estimated from the intersection of multiple range spheres. The accuracy of this estimate is strongly affected by anchor placement and the resulting geometric dilution of precision.[13] To reduce geometric dilution and improve three-dimensional accuracy, anchors should be spatially distributed throughout the operating volume rather than arranged in a nearly coplanar configuration.[13,14] In practice, standalone UWB localization can also experience degraded measurement quality due to non-line-of-sight propagation, multipath effects, and intermittent anchor visibility.[12,13] These effects can reduce the reliability and effective update rate of UWB-only position estimates.

Inertial dead reckoning localizes vehicles by propagating the state from a previous estimate using onboard motion measurements. An onboard Inertial Measurement Unit (IMU) provides high-frequency acceleration and angular-rate data. Linear acceleration can be integrated to estimate velocity and position, while gyroscope measurements can be integrated to estimate vehicle orientation, including roll, pitch, and yaw. This high-rate propagation is useful for maintaining a continuous state estimate between external measurement updates. However, accelerometer and gyroscope noise, bias, and scale-factor errors accumulate through integration, causing drift in the estimated position, velocity, and orientation over time.[15,16] Because this drift grows without bound in the absence of external corrections, standalone inertial dead reckoning is unsuitable for accurate long-duration three-dimensional localization.

Barometric altitude sensing provides an additional lightweight measurement that is particularly useful for vertical estimation. Barometric sensors estimate relative altitude from changes in atmospheric pressure and can provide frequent altitude updates with low mass, low power consumption, and minimal computational cost. Barometric measurements have been shown to improve vertical estimation in UWB-based indoor localization systems when fused through an EKF framework.[18,19] This is especially useful in four-anchor UWB configurations, where vertical accuracy may be limited by anchor geometry and the spatial distribution of anchor heights.

To reduce the inherent limitations of each individual localization technique, this work uses an Extended Kalman Filter (EKF) to fuse UWB, IMU, and barometric measurements. The EKF predicts the vehicle state using inertial dead reckoning and then updates the estimate using UWB range and barometric altitude measurements. In this structure, the IMU provides high-rate state propagation, while the UWB and barometer measurements correct accumulated drift and improve long-term stability. By combining these complementary sensing modalities, the EKF generates an accurate real-time flight path while maintaining compatibility with the inherent constraints of LTA vehicles used in DTR.

III. System Design and Architecture

A lightweight multi-sensor localization system was developed to satisfy the strict payload constraints of the DTR competition while maintaining accurate three-dimensional position estimation. The system integrates UWB ranging, inertial sensing, and barometric altitude measurements within a hardware platform constrained by size and weight. High-rate inertial measurements support continuous state propagation, while UWB and barometric measurements provide drift-bounding corrections.

A. System Architecture

The localization system was designed to minimize weight to remain under the 100 g maximum takeoff weight constraint of the DTR competition. The hardware architecture consists of a Seed Studio XIAO ESP32-S3 microcontroller, a Qorvo DWM1000 UWB transceiver, an Adafruit BNO055 IMU, and an Adafruit BMP280 barometric pressure sensor.

As shown in Fig. 2, the microcontroller coordinates sensor communication and data processing. The DWM1000 UWB module communicates over SPI using the `thotro/arduino-dw1000` library,[20] while the IMU and barometer communicate over a shared I2C bus. This configuration provides a compact interface for heterogeneous sensing while preserving real-time data throughput.

The system operates using a multi-rate sensing architecture. IMU measurements are sampled at 50 Hz, barometric measurements at 20 Hz, and UWB range measurements are incorporated asynchronously as they become available. This structure enables continuous inertial propagation with event-driven correction updates from UWB and barometric measurements. The resulting data flow, illustrated in Fig. 2, supports efficient sensor fusion on payload-constrained platforms.

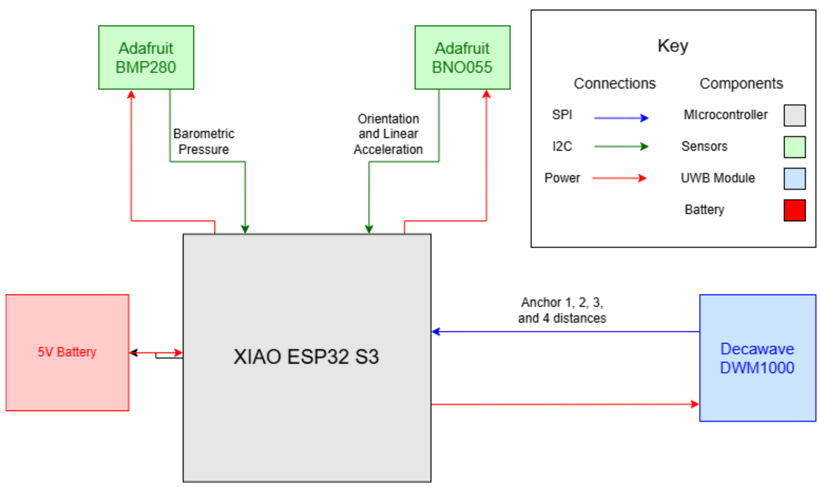

Figure 2. Hardware architecture and data flow of the system.

B. Hardware Integration and Weight Optimization

The complete sensing payload has a mass of 30.17 g. Since the baseline vehicle already includes a XIAO ESP32-S3 microcontroller, IMU, and barometer, integration of the UWB module increases the payload mass by 19.7 g. Several hardware integration strategies were evaluated, as shown in Fig. 3. The initial implementation used a UWB development board to support rapid prototyping, reliable connectivity, and simplified debugging during data collection. Although suitable for validation, this configuration introduces substantial size and weight overhead.

More compact implementations reduce this overhead. A custom PCB integrates a microcontroller and DWM1000 module into a single platform, reducing footprint while maintaining a reliable and serviceable hardware interface. A compact commercial breakout board provides a simpler modular alternative, although with greater packaging overhead than the custom PCB. Direct wire soldering of the DWM1000 module eliminates intermediate boards and connectors, yielding the lowest mass and volume, but increases assembly complexity and reduces accessibility for debugging and maintenance.

These configurations represent a progression from rapid prototyping to flight-ready integration. Direct soldering provides the greatest payload reduction, while custom PCB integration offers the most practical balance between mass, reliability, and maintainability for deployable LTA UAV platforms.

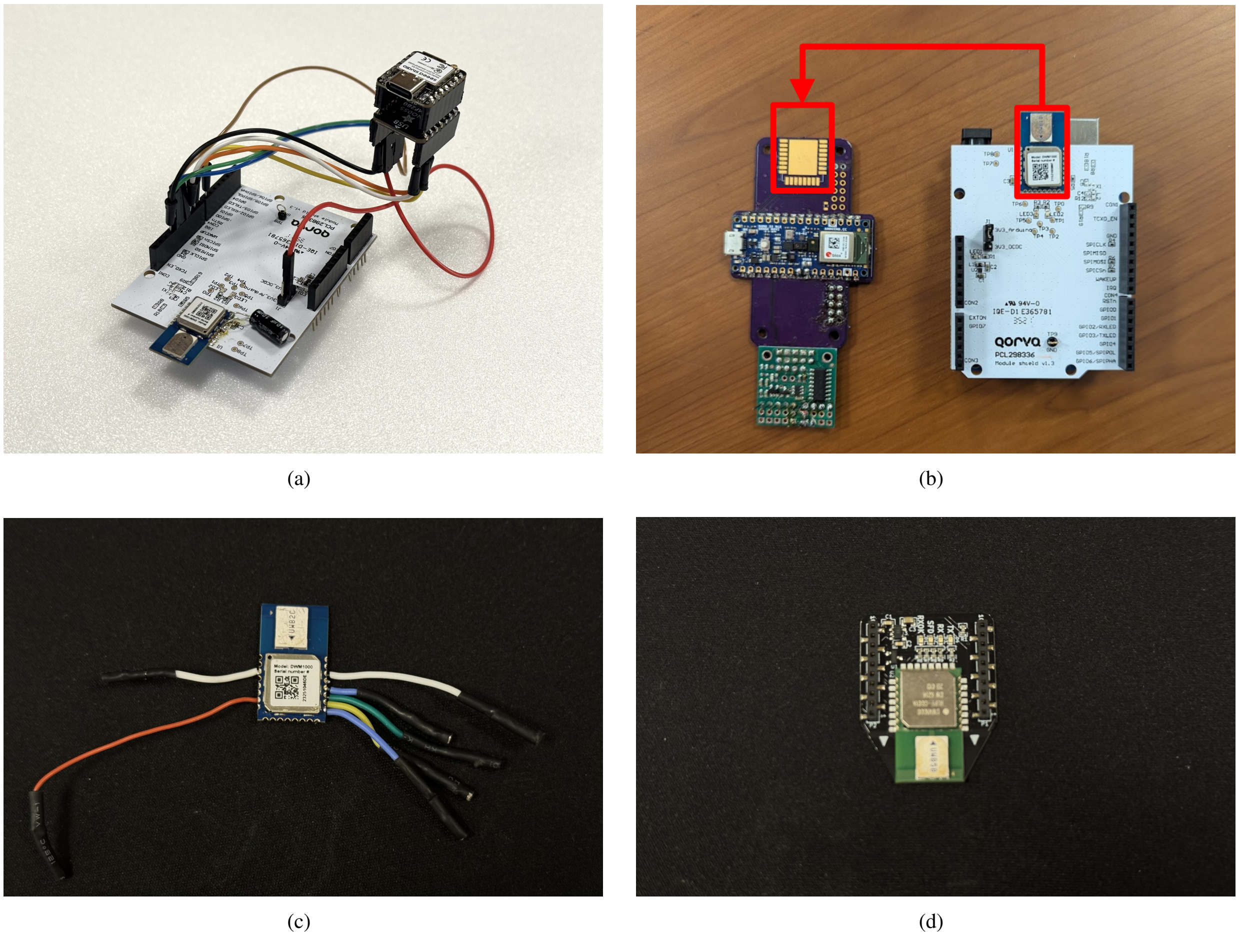

(a) (b) (c) (d)

Figure 3. Hardware integration approaches for the XIAO ESP32-S3, ordered from most to least bulky: (a) full data collection setup with the XIAO ESP32-S3 connected to a Qorvo DWM1000 UWB development board, (b) custom PCB integrating the microcontroller and DWM1000 module, (c) direct wire soldering of the DWM1000 module, and (d) compact commercial breakout board for the DWM1000 module.

C. Localization Method

Three-dimensional localization is performed using an EKF that fuses inertial, UWB, and barometric measurements to estimate vehicle position and velocity. IMU measurements propagate the state between correction updates, while UWB range and barometric altitude measurements bound accumulated drift. UWB updates are applied when new ranges are received, and barometric updates are applied at 20 Hz.

The EKF state vector is defined as

$$\mathbf{x} = \begin{bmatrix} p_x & p_y & p_z & v_x & v_y & v_z \end{bmatrix}^T, \tag{1}$$

where p_x, p_y, and p_z denote position in the global coordinate frame, and v_x, v_y, and v_z denote the corresponding velocity components.

During prediction, the roll, pitch, and yaw angles reported by the IMU are used to transform measured acceleration into the global coordinate frame. The transformed acceleration is integrated using discrete-time kinematics to update the predicted position and velocity. Since inertial dead reckoning accumulates error from sensor noise and bias, the state covariance is propagated during this step to represent increasing prediction uncertainty.[15,16]

When a UWB or barometric measurement is received, the EKF applies the standard measurement-update formulation.[17] Each sensor is represented by a measurement function $h(\mathbf{x})$ that predicts the expected measurement from the current state estimate. The innovation is defined as

$$\mathbf{y}_k = \mathbf{z}_k - h(\mathbf{x}_k^-), \tag{2}$$

where $\mathbf{z}_k$ is the measurement vector and $h(\mathbf{x}_k^-)$ is the predicted measurement evaluated at the predicted state. The Kalman gain then weights prediction uncertainty against measurement uncertainty to update the state estimate and covariance.

For UWB ranging, each anchor provides a scalar distance measurement between the mobile tag and a fixed anchor. For anchor i, with known position $(a_{i,x}, a_{i,y}, a_{i,z})$, the nonlinear measurement function is

$$h_i(\mathbf{x}) = \sqrt{(p_x - a_{i,x})^2 + (p_y - a_{i,y})^2 + (p_z - a_{i,z})^2}. \tag{3}$$

The corresponding UWB innovation is

$$y_{k,i} = z_{uwb,i} - h_i(\mathbf{x}_k^-), \tag{4}$$

where $z_{uwb,i}$ is the measured range from anchor i. Because the UWB measurement is nonlinear and radial, the EKF linearizes the measurement model about the predicted state using the Jacobian.[17,18] For anchor i, the UWB measurement Jacobian is

$$\mathbf{H}_{uwb,i} = \begin{bmatrix} \frac{p_x - a_{i,x}}{h_i(\mathbf{x})} & \frac{p_y - a_{i,y}}{h_i(\mathbf{x})} & \frac{p_z - a_{i,z}}{h_i(\mathbf{x})} & 0 & 0 & 0 \end{bmatrix}. \tag{5}$$

This Jacobian maps the scalar range innovation into the Cartesian position states along the direction between the predicted tag location and the anchor. When multiple valid UWB ranges are available in a packet, the corresponding measurement functions and Jacobian rows are assembled into a single EKF update. This allows partial UWB packets to contribute to the estimate without requiring simultaneous valid ranges from all anchors. Measurements marked as stale or containing non-positive ranges are rejected before the update step.

Barometric altitude is incorporated as a direct measurement of the vertical position state. The barometric measurement function is

$$h_{baro}(\mathbf{x}) = p_z. \tag{6}$$

The barometric innovation is

$$y_{k,baro} = z_{baro} - p_z, \tag{7}$$

where z_{baro} is the measured barometric altitude. The corresponding measurement matrix is

$$\mathbf{H}_{baro} = \begin{bmatrix} 0 & 0 & 1 & 0 & 0 & 0 \end{bmatrix}. \tag{8}$$

This update directly constrains vertical position and reduces altitude drift caused by inertial integration.

Barometric correction is particularly important because the system uses only four UWB anchors. Although four anchors are sufficient for three-dimensional trilateration, localization accuracy depends strongly on anchor geometry, geometric dilution of precision, and the distribution of anchor heights.[13,14] Prior work has also shown that barometric measurements can improve vertical estimation in UWB-based indoor localization when fused through an EKF.[18,19] In this implementation, the barometric measurement noise parameter was set to $\sigma_{baro} = 0.01$, causing the EKF to strongly weight altitude measurements during vertical updates while retaining UWB corrections for the full three-dimensional position estimate.

D. Testing Environment and Ground Truth Validation

A controlled kinematic test was conducted to validate the sensor fusion architecture. Four stationary UWB anchors were placed at known locations around the test environment to reduce geometric dilution of precision and improve three-dimensional localization accuracy.[13,14] The anchor coordinates, in meters, were

- Anchor 1: $(15.5, 0.0, 1.83)$
- Anchor 2: $(0.0, 8.8, 7.2)$
- Anchor 3: $(0.0, 0.0, 0.0)$
- Anchor 4: $(15.5, 10.0, 4.5)$

To establish a repeatable reference trajectory, the UWB tag and sensor payload were mounted to a rigid pole and manually moved along a circular path with a radius of 3.35 m centered at $(6.7, 4.9)$. During the test, the tag altitude was varied between 2.0 m and 3.5 m above the ground plane. This controlled three-dimensional trajectory served as the baseline for comparison with the EKF-generated position estimates. The test configuration is shown in Fig. 4.

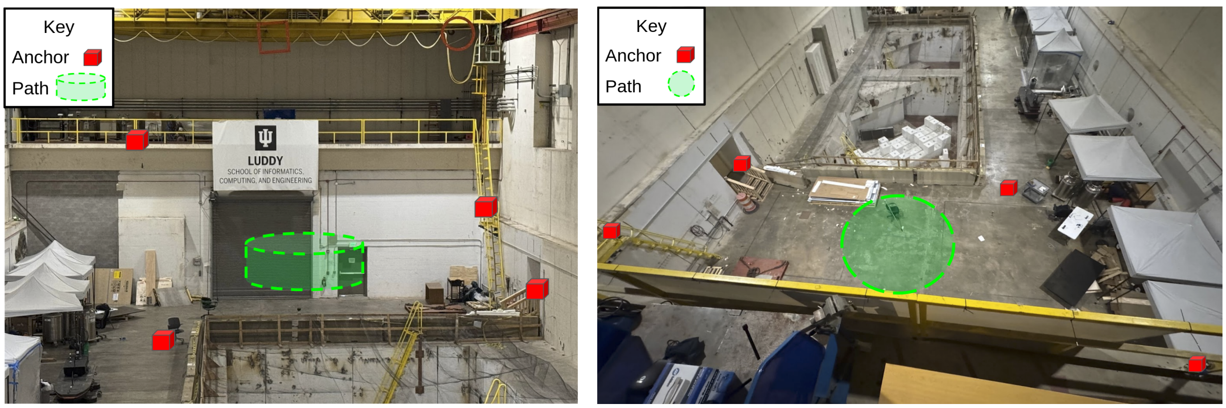

(a)

(b)

Figure 4. Testing setup in the MESH building at Indiana University: (a) full view of the environment with anchor placements, and (b) bird's-eye view of the test area and trajectory region.

IV. Results and Discussion

The proposed three-dimensional localization system was evaluated by comparing the EKF-estimated trajectory with the prescribed test path described in the methodology. Since time-synchronized absolute ground truth was not collected, the reported errors represent deviations from the expected trajectory and altitude bounds rather than absolute localization error. Performance was evaluated using horizontal radial error, vertical bound error, and a combined three-dimensional trajectory-bound error.

A. Horizontal Tracking Performance

Horizontal tracking was evaluated by comparing the EKF-estimated position in the XY plane with the prescribed circular path. The radial error was defined as the absolute difference between the estimated distance from the circle center and the expected radius:

$$e_{xy} = \left| \sqrt{(p_x - C_x)^2 + (p_y - C_y)^2} - r \right|, \tag{9}$$

where (C_x, C_y) is the circle center and r is the prescribed radius.

As shown in Fig. 5, the estimated trajectory closely follows the expected circular path after filter convergence. The system achieved a mean radial error of 0.324 m and an RMSE radial error of 0.345 m. The maximum radial error was 1.745 m and occurred during the initial convergence period. Following this transient, the trajectory remained tightly bounded around the prescribed path, indicating that UWB range updates effectively constrained horizontal drift from inertial propagation.

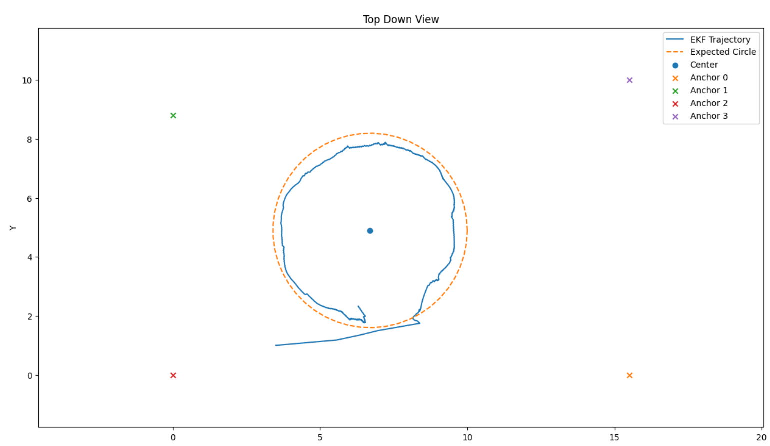

Figure 5. Top-down view of the EKF-estimated trajectory compared to the prescribed circular path.

B. Vertical Tracking Performance

Vertical tracking was evaluated using the expected altitude envelope of the test trajectory. During the experiment, the system was manually moved between approximate altitude bounds of 2.0 m and 3.5 m. Since time-synchronized vertical ground truth was not collected, vertical performance was quantified using a bound-error metric rather than absolute altitude error:

$$e_z = \begin{cases} Z_{min} - p_z, & p_z < Z_{min} \\ p_z - Z_{max}, & p_z > Z_{max} \\ 0, & Z_{min} \le p_z \le Z_{max} \end{cases} \tag{10}$$

where Z_{min} and Z_{max} define the expected altitude range.

As shown in Fig. 6, the EKF estimate remained within the expected altitude bounds for most of the test. The mean vertical bound error was 0.010 m, and the maximum vertical bound error was 1.000 m during the initial convergence period. The low mean bound error indicates that the barometric update strongly constrained vertical drift. However, because this metric only measures deviations outside the expected altitude envelope, it should not be interpreted as centimeter-level absolute altitude accuracy.

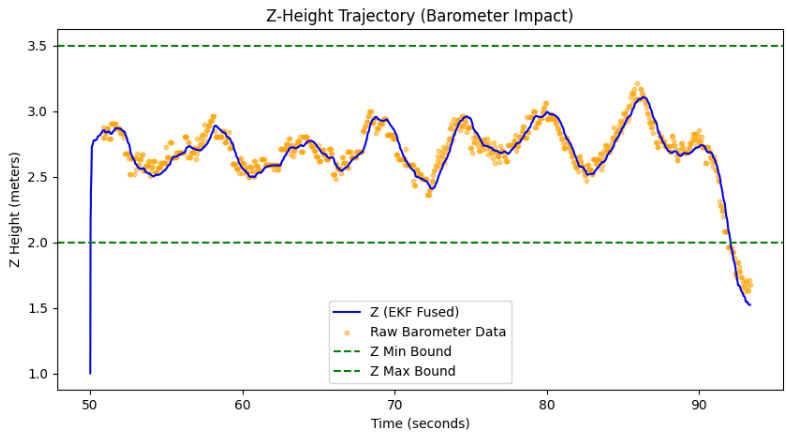

Figure 6. Estimated vertical trajectory with raw barometric measurements and expected altitude bounds.

C. Combined Trajectory-Bound Error

To summarize boundedness in three dimensions, a combined trajectory-bound error was computed from the horizontal radial error and vertical bound error:

$$e_{3D} = \sqrt{e_{xy}^2 + e_z^2}. \tag{11}$$

This metric captures deviation from the prescribed circular path in the horizontal plane and deviation outside the expected altitude envelope. It does not represent absolute Euclidean error from a time-synchronized three-dimensional ground-truth trajectory.

Using this metric, the EKF achieved a mean combined trajectory-bound error of 0.327 m. Figure 7 shows the horizontal radial error, vertical bound error, and combined trajectory-bound error over time. The horizontal radial component dominated the combined error, while the vertical bound error remained near zero for most of the trajectory. The largest errors occurred at the beginning of the test during filter initialization and convergence. After convergence, the filter maintained a stable bounded estimate for the remainder of the trajectory.

D. Three-Dimensional Trajectory

The estimated three-dimensional trajectory is shown in Fig. 8. After the initial convergence period, the trajectory remained largely within the prescribed cylindrical test region. This result indicates that the proposed UWB, IMU, and barometer fusion approach can maintain a bounded three-dimensional position estimate in a controlled indoor environment using only four UWB anchors. The barometer improved vertical boundedness, while UWB range measurements constrained horizontal drift and corrected accumulated inertial error.

These results demonstrate promising localization performance under size, weight, and power constraints. However, the test trajectory was defined geometrically rather than measured using an independent motion-capture or surveying system. Therefore, the reported metrics should be interpreted as prescribed-path deviations rather than absolute localization accuracy. Future work will improve upon this design to better estimate ground truth altitude and positional information.

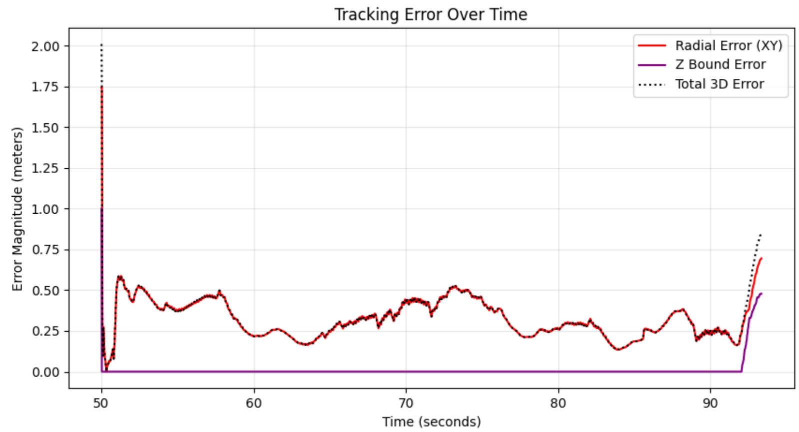

Figure 7. Tracking error over time, including horizontal radial error, vertical bound error, and combined trajectory-bound error.

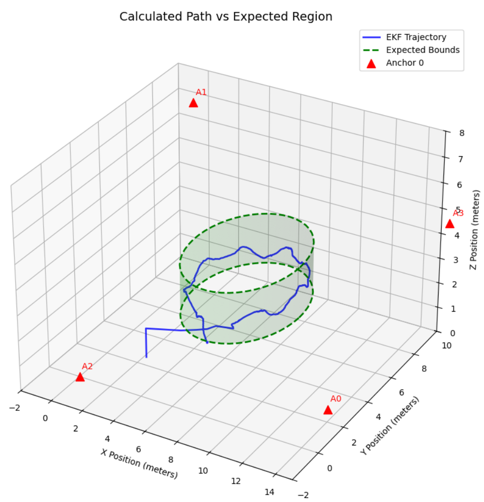

Figure 8. EKF-estimated 3D trajectory compared to the prescribed cylindrical test region.

V. Conclusion and Future Work

This paper presented a lightweight, low-cost multi-sensor fusion architecture for GPS-denied localization of lighter-than-air unmanned aerial systems. The system was designed to satisfy the size, weight, power, and cost constraints of the Defend the Republic competition while providing localization performance suitable for fleet coordination and autonomous goal scoring. The proposed architecture fuses UWB ranging, inertial measurements, and barometric altitude measurements using an EKF. In this framework, IMU measurements provide continuous state propagation, while UWB and barometric measurements correct drift accumulated through inertial dead reckoning.

Experimental testing evaluated localization performance by comparing the EKF-estimated trajectory with a prescribed test path. The fused solution achieved a mean horizontal radial error of 0.324 m, a mean vertical bound error of 0.010 m, and a mean combined trajectory-bound error of 0.327 m. These results indicate that the proposed sensor-fusion approach can maintain a bounded sub-meter position estimate in a GPS-denied indoor environment. The EKF architecture improved trajectory consistency by combining complementary sensor modalities and reducing the drift associated with individual UWB sensors.

The complete localization payload had a total mass of 30.17 g and an estimated cost of $165. Since the baseline vehicle already includes the microcontroller, IMU, and barometer, the UWB module adds only 19.7 g of additional payload mass. Further mass reduction will be pursued through a custom PCB optimized for LTA UAV payload constraints, including tighter component integration and connector elimination.

Future work will focus on hardware refinement, expanded validation, and mission-level integration. The current experiments used a manually moved payload rather than a free-flying LTA UAV; therefore, future testing should include onboard flight experiments with time-synchronized external ground truth, such as motion-capture or surveyed reference data. Additional evaluation should compare the fused EKF solution against UWB-only and IMU-only baselines to quantify the contribution of each sensing modality.

For the DTR competition, the localization system will be integrated with fleet coordination, path planning, and autonomous scoring algorithms. The proposed three-dimensional localization approach can support high-speed vehicles without onboard cameras by allowing them to localize relative to the arena while receiving game-ball coordinates from vision-equipped teammates. This architecture enables camera-free vehicles to participate in autonomous scoring while reducing payload complexity.

Acknowledgments

The fourth author gratefully acknowledges support from the NSWC Crane Naval Innovation Science & Engineering (NISE) Program, the ONR Independent Applied Research (IAR) Program, and the DoW Science, Mathematics, and Research for Transformation (SMART) Scholarship-for-Service Program.

References

[1] Indiana University, Aerospace Systems Lab, "Defend The Republic Fall 2024," `https://www.iu-dtr.com/`.

[2] George Mason University, Patriot Pilots, "Defend The Republic Spring 2025," `https://gmublimpsquad.github.io/index.html`.

[3] Taylor, C., Widjaja, M., and Deters, R. W., "Remotely-Processed Vision-Based Control of Autonomous Lighter-Than-Air UAVs with Real-Time Constraints," AIAA SciTech Forum 2025, Orlando, FL. 2025.

[4] Meighan, A., Taylor, C., and Dantsker, O., "Multi-Modality Localization of Autonomous Lighter-Than-Air UAVs in Real-Time," AIAA Paper 2026-0858, AIAA SciTech Forum 2026, Orlando, FL.

[5] Guanghui, X., Ruixue, L., Zhenghao, Z., and Rui, L., "State-of-the-art and Tendency of SLAM Algorithms Based on 3D LiDAR," *INFORMATION AND CONTROL*, Vol. 52, No. 1, 2023, pp. 18–36.

[6] Messinger, S., *Modeling, Adaptive Control, and Flight Testing of a Lighter-than-Air Vehicle Validated Using System Identification*, Master's thesis, The Pennsylvania State University, 2022, Master's Thesis.

[7] Mathew, J. P., Karri, D., Yang, J., Zhu, K., Gautam, Y., Nojima-Schmunk, K., Shishika, D., Yao, N., and Nowzari, C., "Lighter-Than-Air Autonomous Ball Capture and Scoring Robot – Design, Development, and Deployment," *arXiv preprint arXiv:2309.06352*, 2023.

[8] Taylor, C. and Dantsker, O. D., "Lighter-Than-Air Vehicle Design for Target Scoring in Adversarial Conditions," AIAA Paper 2024-3896, AIAA Aviation Forum 2024, Las Vegas, NV. 2024.

[9] Taylor, C. and Dantsker, O. D., "Lighter-Than-Air-Vehicle Design for Adversarial Defense," AIAA Paper 2025-3124, AIAA Aviation Forum 2025, Las Vegas, NV. 2025.

[10] Xu, J., D'antonio, D. S., Ammirato, D. J., and Saldaña, D., "SBlimp: Design, Model, and Translational Motion Control for a Swing-Blimp," *2023 IEEE/RSJ International Conference on Intelligent Robots and Systems (IROS)*, IEEE, 2023, pp. 6977–6982.

[11] Qorvo, "DWM1000 3.5 - 6.5 GHz Ultra-Wideband (UWB) Transceiver Module," https://www.qorvo.com/products/p/DWM1000.

[12] Alarifi, A., Al-Salman, A., Alsaleh, M., Alnafessah, A., Al-Hadhrami, S., Al-Ammar, M. A., and Al-Khalifa, H. S., "Ultra Wideband Indoor Positioning Technologies: Analysis and Recent Advances," *Sensors*, Vol. 16, No. 5, 2016, pp. 707.

[13] Bach, S.-H. and Yi, S.-Y., "Constrained Least-Squares Trilateration for Indoor Positioning System Under High GDOP Condition," *IEEE Transactions on Industrial Informatics*, Vol. 20, No. 3, March 2024, pp. 4550–4558.

[14] Cho, J. and Lee, B., "Optimal layout of four anchors to improve accuracy of Ultra-Wide band based indoor positioning," *Expert Systems with Applications*, Vol. 255, 2024, pp. 124808.

[15] Barshan, B. and Durrant-Whyte, H. F., "Inertial Navigation Systems for Mobile Robots," *IEEE Transactions on Robotics and Automation*, Vol. 11, No. 3, 1995, pp. 328–342.

[16] Blum, C. and Dambeck, J., "Analytical Assessment of the Propagation of Colored Sensor Noise in Strapdown Inertial Navigation," *Sensors*, Vol. 20, No. 23, 2020.

[17] Welch, G., Bishop, G., et al., "An introduction to the Kalman filter," 1995.

[18] Zhang, M., Vydhyanathan, A., Young, A., and Luinge, H., "Robust height tracking by proper accounting of nonlinearities in an integrated UWB/MEMS-based-IMU/baro system," *Proceedings of the 2012 IEEE/ION Position, Location and Navigation Symposium*, 2012, pp. 414–421.

[19] Li, J., Wang, Y., Chen, Z., Ma, L., and Yan, S., "Improved Height Estimation Using Extended Kalman Filter on UWB-Barometer 3D Indoor Positioning System," *Wireless Communications and Mobile Computing*, Vol. 2021, No. 1, 2021, pp. 7057513.

[20] Trojer, T., "arduino-dw1000: A library that offers functionality to use Decawave's DW1000," 2019, Available: `https://github.com/thotro/arduino-dw1000`. Accessed: May 5, 2026.